RSC Advances

This is an *Accepted Manuscript*, which has been through the Royal Society of Chemistry peer review process and has been accepted for publication.

Accepted Manuscripts are published online shortly after acceptance, before technical editing, formatting and proof reading. Using this free service, authors can make their results available to the community, in citable form, before we publish the edited article. This *Accepted Manuscript* will be replaced by the edited, formatted and paginated article as soon as this is available.

You can find more information about *Accepted Manuscripts* in the Information for Authors.

Please note that technical editing may introduce minor changes to the text and/or graphics, which may alter content. The journal's standard Terms & Conditions and the Ethical guidelines still apply. In no event shall the Royal Society of Chemistry be held responsible for any errors or omissions in this *Accepted Manuscript* or any consequences arising from the use of any information it contains.

ROYAL SOCIETY OF CHEMISTRY

www.rsc.org/advances

RSC Advances RSCPublishing

ARTICLE

Cite this: DOI: 10.1039/x0xx00000x

Received 00th, December 2014
Accepted 00th

DOI: 10.1039/x0xx00000x

www.rsc.org/

A New Injectable Biphasic Hydrogel Based on Partially Hydrolyzed Polyacrylamide and Nanohydroxyapatite, as Scaffold for Osteochondral Regeneration

Newsha. Koushki[a,b], Ali Asghar Katbab[a,*], Hossein Tavassoli[b], Mohammad Majidi[b], Azadeh Jahanbakhsh[b] and Shahin Bonakdar[b,*]

[a] Polymer Engineering and Color Technology Department, Amirkabir University of Technology, Tehran, Iran
[b] National Cell Bank of Iran, Pasteur Institute of Iran, Tehran, Iran
[*] Corresponding author: Tel.: +98 21 644 18107; Fax: +98 21 664 69162. katbab@aut.ac.ir , (A.A. Katbab). Tel. +98 21 66953311; Fax +98 21 66465132. sh_bonakdar@pasteur.ac.ir , (Sh. Bonakdar).

Attempts have been made to fabricate an injectable biphasic hydrogel based on partially hydrolyzed polyacrylamide (HPAM), nanocrystalline hydroxyapatite (nHAp), and chromium acetate (Cr (III)) as crosslink agent as a novel scaffold for osteochondral repair. The HPAM water solution comprising 4 wt. % HPAM and 0.2 wt. % Cr (III) (HPAM3) and its counterpart containing 50 wt. % nHAp showed to be optimized in vial titling method and cell viability assays. The biphasic hydrogel demonstrated high interfacial attraction by performing tensile test measurement. The Rheo-mechanical analysis performed on the prepared hydrogels revealed that incorporation of 50 wt. % of nHAp (HPAM6) not only reinforced the mechanical strength of the final crosslinked gel, but lowered the gelation onset as well as gelling time. Atomic force microscopy (AFM) characterization together with water uptake measurement showed that an increase in crosslink density enhanced surface elasticity as well as reduced equilibrium swelling degree. The engineered constructs (HPAM3 and HPAM6) also supported cell attachment as indicated by SEM observation. Alcian blue, safranin O and dimethyl methylene blue indicated chondrogenic phenotype in the HPAM3 constructs with the highest amount after 21 days of culture. Chondrogenic differentiation of mesenchymal stem cells (MSCs) in the HPAM3 was evident by real-time PCR analysis for cartilage-specific ECM gene markers. Interestingly, in Real-time PCR analysis for bone-specific ECM gene markers, up-regulated expression of osteogenic genes was related to osteoblastic differentiation of encapsulated MSCs within HPAM/nHAp scaffolds, as confirmed by calcium deposition. The results suggested that our designed biphasic hydrogel has potential to be considered as a promising scaffold for osteochondral regeneration.

Keywords: Partially hydrolyzed polyacrylamide, nanocrystalline hydroxyapatite, chromium acetate, injectable biphasic hydrogel, osteochondral

RSC Advances Accepted Manuscript

1. Introduction

Cartilage predominantly contains extracellular matrix (ECM) proteins, primarily Col II and Aggrecan, which determine the tissue's stability and mechanical strength.[1] Articular cartilage defects are mainly resulted from the tissue deficiency with age, diseases and traumas.[2] However, articular cartilage has a weak intrinsic healing capacity due to its avascular nature and lack of cellular migration to the sites of cartilage injury.[2] As a result, even a small chondral defect may permeate so extensively through the joint that it may lead to the smooth lining of the articulating surface and the underlying subchondral bone.[3,4] Hence, Bone and cartilage tissue engineering remain as significant challenges in the area of orthopedic surgery.[3, 4] There are numerous therapeutic options applied for cartilage and bone restoration,[5-7] but a lot of these surgical techniques have not been efficient. Tissue engineering has been emerged as a potential alternative to promote the quality of the cartilage

and bone repair.[8, 9] Hydrogels, as three-dimensional (3D) scaffolds, mimic in vivo condition and enable the incorporated cells to form relevant tissue spheroids.[10-12] Moreover, hydrogels can be designed as injectable forms and utilized in minimally invasive methods.[13,14] However, weak mechanical properties of injectable hydrogels restrict their applications to drug delivery and soft tissue repair.[14-16] Nanocomposite hydrogels have overcome some of these limitations, and using nHAp as a main predominant component of the calcified tissues has been proposed because of its biocompatibility and osteoconductive capability.[17-19] Recently, hydrogel systems comprising biphasic structure with potential for early stage osteochondral defect repair have been also studied and shown good capacity for healing both damaged cartilage and underlying subchondral bone.[20, 21]

The extent of effectiveness and suitability of a polymer based hydrogel system for tissue engineering purposes is governed by the type of the used polymer, type of crosslink agent and crosslinking characteristics. Partially hydrolyzed Polyacrylamide seems to have a good potential for this purpose and has been studied for the first time in the present work. HPAM is a synthetic water soluble polymer comprising both carboxylate (-COO-) and amide (-CONH2) as side groups attached to the backbone of the polymer chains.[22] The extent of water solubility, mechanical properties and crosslinkability of this polymer can be tailored by molecular weight and the carboxylate to amide group ratio. However, it is well believed that the properties of natural polymers such as alginate depend on the source of isolation, and alterations in these properties are limited to the initial source and are not tunable. Furthermore, the presence of free carboxylate groups on the HPAM structure makes it suitable for conjugation of bio-molecules to modulate cell adhesion, proliferation and differentiation.[23] HPAM hydrogel networks can be also formed as a result of ionic crosslinking in the presence of divalent or trivalent metals, which eliminates the need for photo initiators, UV radiation and free radical reactions that are detrimental to cells. Moreover, as the injectability and gelation time of HPAM system are well tunable, it can be used as injectable scaffold, whereas certain natural polymers such as alginate system could not be utilized in injectable forms due to the rapid gelation. The transparency of HPAM system as well as easily sterilized by autoclave without any problem for denaturation is other advantages of it over some other systems. In the present work, attempts have been made to employ HPAM for the preparation of an injectable and biodegradable hydrogel as a scaffold for early stage osteochondral regeneration. A biphasic hydrogel including one phase composed of HPAM and chromium acetate as crosslink agent to promote cartilage regeneration, and second phase with similar composition and containing nHAp to provide integration to subchondral bone as well as osteogenic differentiation was applied. The properties of the prepared hydrogels such as gelation time, water uptake, degradation, mechanical strength, biocompatibility, cell attachment and differentiation were also studied.

2. Experimental

2.1. Materials

Water soluble partially hydrolyzed polyacrylamide powder with the hydrolysis degree of 20–25% and average molecular weight of 12×106 Dalton was provided by SNF Company (France) with the commercial name of FlOPAAm 2430. Chromium acetate powder as a crosslink agent was purchased from Alfa Aesar Company (USA). Nanohydroxyapatite was also synthesized according to the chemical precipitation method as previously reported.[24]

2.2. Preparation and Optimization of hydrogels

HPAM powder was dissolved in deionized water and sterilized in autoclave. The solution was kept overnight at 25 °C so that the HPAM chains could obtain their equilibrium conformation. Cr (III) aqueous solution as a crosslink agent with predetermined concentration was filtered (0.2 µm) and mixed with the HPAM solution. To accelerate the gelation of the HPAM solutions at 37 °C, the prepared hydrogel solutions were first preheated at 60 °C while still remained injectable. Biphasic structure was prepared using optimized hydrogel solutions containing 0 and 50 wt. % nHAp. The preparation route of the biphasic hydrogel has been schematically demonstrated in Fig. 1. All the designed formulations for various steps of the work are illustrated in Table 1 (See supporting information for more detail (S-I)).

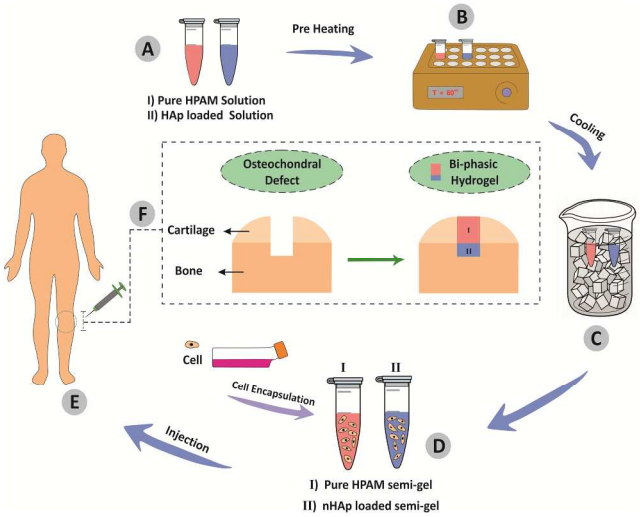

Fig. 1 A-E) Total steps from hydrogel preparation to injection in osteochondral site, F) magnification of injection of biphasic HPAM hydrogel into osteochondral lesion.

Table 1. Composition of the designed hydrogel systems.

Sample Code	HPAM Concentration (wt. %)	Cr(III) Concentration (wt. %)	nHAp (wt. %)
HPAM1	4	0.06	0
HPAM2	4	0.1	0
HPAM3	4	0.2	0
HPAM4	4	0.3	0
HPAM5	4	0.4	0
HPAM6	4	0.2	50

2.3. Structural characterization

2.3.1. Tensile test measurement. To measure the strength of the interface between the two phases, tensile test was done in triplicate on the prepared biphasic samples using a tensile testing machine model GAIDABINI (SUN 2500, England), and the average value

RSC Advances Accepted Manuscript

was reported. The test was performed on cylindrical shaped samples with the tensile rate of 5 mm/min at 27 °C (ambient temperature).

2.3.2. Rheological analysis. The onset and rate of gelation process of the HPAM solutions comprising crosslink agent were followed by performing Rheological analysis using a Paar Physica Rheometer model UDS 200 with cone and plate (50 mm diameter) configuration in oscillatory mode. For this purpose, 0.5 ml of the preheated HPAM3 solution was prepared and immediately loaded onto the rheometer at 37 °C. The upper plate was lowered to a gap size of 0.5 mm simultaneously, and the measurement started. The sample solution was subjected to the dynamic amplitude of 1% with frequency of 0.1 Hz. The measurement proceeded until the ultimate modulus of the crosslinked hydrogel reached to a constant level. In addition, crosslink density of the hydrogel network (ν_{RH}) was calculated according to the ν_{RH}= G'/R where G′ is the ultimate modulus, R is the gas constant (8.314 Jmol-1K-1) and T represents the test temperature (310.15K). [25]

2.3.3. Atomic force microscopy analysis. As the gel surface stiffness plays as a key control in cell attachment and proliferation, the surface elastic modulus of the hydrogels as a function of crosslink density was evaluated using Atomic force microscopy model nano wizard II, JPK (Germany) equipped with conically tipped cantilever with a nominal spring constant of 0.12 N/m. Each hydrogel sample was prepared on a glass slide and incubated in phosphate buffered saline (PBS, Sigma, USA) to represent the biological environment. The elastic modulus was obtained according to the following equation by fitting data from a plot of cantilever deflection versus piezo displacement to a conic Hertz model by the method described in previous reports.[26]

$$E=\frac{F(1-\upsilon^2)\pi}{2\delta^2\tan\alpha} \quad (1)$$

2.3.4. Water uptake and gel content measurement. To evaluate the degree of water uptake, the crosslinked hydrogel samples with the specific dimensions (height= 10mm, diameter= 5mm) were accurately weighed (W_0) and immersed in 5 ml water solution at 37 °C. The samples were re-weighed at regular time intervals (W_s) to find the equilibrium swelling. The water uptake was defined as (W_s-W_0) ×100/W_s. To evaluate the potential of the hydrogels for disintegration when subjected to the body biological fluid, the weight loss of the samples after equilibrium swelling was followed to determine the rate of dissolution. The weight of samples at the regular time intervals (W_t) and the initial weight (W_0) were used to calculate the percent of remaining gel according to the W_t×100/W_0.

2.4. Cell culture

Adipose derived mesenchymal stem cells (MSCs) and articular cartilage chondorcytes were freshly provided by National Cell Bank, Pasteur Institute of Tehran (Iran). The cells were cultured in Dulbecco's Modified Eagles' Medium (DMEM, GIBCO, Scotland)/Ham's F12 (GIBCO, Scotland) supplemented with 10% fetal bovine serum (FBS, Nanobioarray, Iran).[27]
To perform cell encapsulation, prepared hydrogel precursors were subjected to preheating and cooling prior to the incorporation of cell suspension into each hydrogel solution to achieve the final solution containing 50% culture medium. The solutions were then gently mixed and allowed to be completely gelled at 37 °C. Afterwards, the culture medium was added on top of each hydrogel, and the samples were incubated at 37 °C with refreshing the medium every 3 days.

2.5. In vitro evaluation tests

To assess the possible toxic effect of Cr (III) solution as crosslink agent of the hydrogels, amino-7-dimethylamino-2-methyl-phenazine hydrochloride (neutral red, Sigma) assay was employed.[28] The viability of the encapsulated MSCs was followed by agar diffusion protocol according to the standard ISO 10993 (see supporting information (S-II)).[29] The morphology of the MSCs encapsulated in the optimized hydrogels (HPAM3 and HPAM6) was also viewed using scanning electron microscope (SEM) model HITACH S4160 (Japan), at voltage 15 KV.

2.6. Functional assessment

Proteoglycan expression was stained by Alcian blue and safranin O specific dyes, [30] and quantified using dimethyl methylene blue (DMMB) procedure [11] to evaluate the chondrogenic potential of the optimized hydrogel sample (HPAM3). For osteogenicity of the encapsulated cells within HPAM6, the presence of calcium was quantified using Alizarin Red staining protocol (for more detail see supporting information (S-III)).[31, 32]

2.7. Real Time- PCR analysis

Gene expression of encapsulated MSCs was analyzed in two different groups as follows: 1) stem cells and chondrocytes encapsulated in the HPAM3, 2) stem cells incorporated into the HPAM6. Mono layer cultured cells also considered as control in each group. The cells with the density of 1×105 were cultured for 21 days with the medium exchange of every 3 days. Real Time-PCR was performed using SYBR Premix Ex Taq II master mix (TaKaRa) with 7 specific primers provided in Supplementary Table S-IV.1 on One Step instrument (applied biosystem). For chondrogenic differentiation, GAPDH was used as endogenous control, and for osteogenic differentiation all samples were normalized to Col I (see supporting information for more detail (S-IV)).

2.8. Statistical analysis

All data were reported as mean ± standard deviation, and each experiment was done in triplicate. One-way analysis of variance (ANOVA) was applied to compare various groups and p value< 0.05 was considered to be statistically significant.

3. Results

In Figures 2A and B the effects of HPAM concentration as well as Cr (III) level upon the kinetic of gelation process has been illustrated. It can be observed in Fig. 2A that increasing the polymer concentration leads to the reduction of gelation time at 60 °C. The optimum polymer concentration found to be around 4 wt. % with a total gelation time of 8 minutes at 60 °C in the presence of 0.2 wt. % Cr (III). Although higher amounts of Cr (III) led to the faster gelation (Fig. 2B) and higher stiffness, Cr (III) solutions with high concentrations showed cytotoxic effect upon the cultured cells and decrease in cell compatibility. Therefore, the HPAM3 solution comprising 4 wt. % HPAM and 0.2 wt. % Cr (III) found to be optimized. Furthermore, as the designed HPAM hydrogel system was also aimed to be employed as scaffold for subchondral bone regeneration purpose, samples with various level of nHAp were synthesized to obtain the optimized concentration from the bioactivity,

RSC Advances Accepted Manuscript

mechanical strength as well as injectability points of views. Above 50 wt. %, nHAp particles could not completely disperse in HPAM water solution, and precipitation of the nHAp particles occurred, whereas below 50 wt. %, monodispersion of nHAp particles was observed. However, the crosslinked hydrogel samples prepared by low concentration of nHAp exhibited bioactivity and mechanical strength lower than the sample originated with 50 wt. % nHAp. Hence, 50 wt. % of nHAp found to be an optimized level for the nHAp filled hydrogel phase.

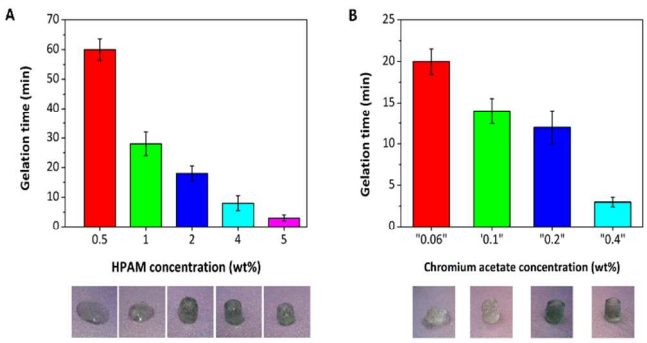

Fig. 2 Gelation time of HPAM/Cr (III) solutions at 60 °C with A) different HPAM concentrations and 0.2 wt. % Cr (III), B) 4wt. % HPAM and various Cr (III) concentrations. Error bars represent means ± standard deviation for n=3.

The results of test tube inverting method showed that HPAM3 and HPAM6 as the most suitable hydrogel precursors remained still injectable after being subjected to preheating at 60 °C for 2 and 1 minutes respectively. After cell encapsulation and incubation at 37 °C, both the preheated solutions were transformed into a completely crosslinked network after 30 and 20 minutes, respectively, which seemed to be appropriate gelation time for an injectable hydrogel system. However, short gelation time is not suitable, as it would not permit the hydrogel solutions to be injected. Very long gelling time is also not satisfactory, as it would take a long time for the precursors to start crosslinking and gelation after being injected. Hence, the gelling time of 30 and 18 minutes for the HPAM3 and its counterpart without nHAp were supposed to be acceptable. The sample with biphasic structure was prepared by the addition of aqueous solution of HPAM3 to HPAM6 after preheating and cell encapsulation. Fig. 3 illustrates the mechanism of the gelation process schematically, and the final biphasic sample which demonstrates integration at the interface with the transparent and opaque appearance in HPAM3 (pure hydrogel) and HPAM6 (nanocrystalline loaded hydrogel) parts, respectively. The bonding between HPAM aqueous solution (the first phase) and HPAM/nHAp water solution (the second phase) is occurred due to the inter-diffusion of both phases and crosslinking at the interface. In fact, due to the preheating of the two phases, the high viscosity hindered them to completely flow into each other before fulfilment of the crosslinking. However, they were in contact with each other only at the interface in the way that HPAM6 phase was prepared in the mold and the HPAM3 solution was overlaid on the prior phase. As both phases had crosslink agent, they were interlocked via crosslinking, leading to a high interfacial attraction between the two phases. This was confirmed by performing tensile test on the prepared biphasic samples to quantified strength of the interface between two phases. The samples showed 550% elongation with 262.8 kPa stress at the break point, indicating good extensibility. The samples were broken from the phase without nHAp but not within the interface. This demonstrates the intensified interface between the two phases which is explained to be due to the interlocking of the polymer segments at the interface. The time was set in a way that the two phases linked together before fulfilment of gelation of each phase. In order to utilize this biphasic structure for articular cartilage repair, the HPAM/nHAp phase must be injected into the bone and the second phase injected after that. The bonding between these two phases also eliminates the suturing.

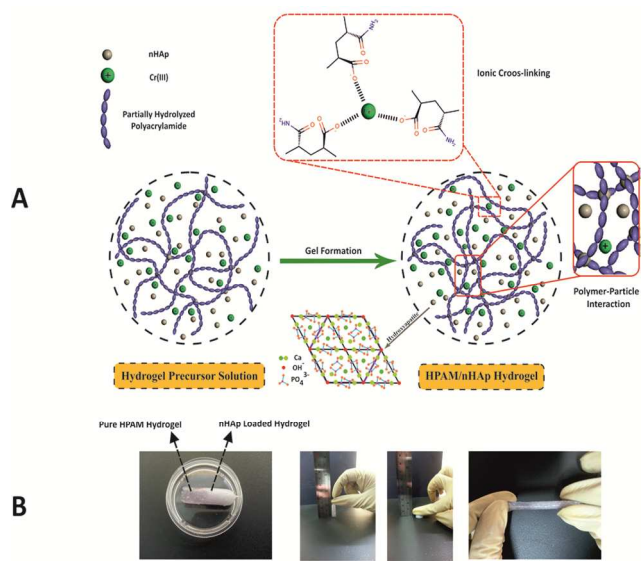

Fig. 3 A) Mechanism of the gelation of HPAM/nHAp containing 50 wt. % nHAp and 0.2 wt. % Cr (III), B) Loading and unloading of the biphasic hydrogel.

The rheological parameters showed the initial constant storage modulus higher than loss modulus for both optimized preheated gelant solutions at the beginning of the test (induction time), indicating the presence of physical network as a result of high molecular weight of the polymer and physical entanglements between the polymer segments. After that the dynamic elastic modulus (G') of the samples increased by time due to the occurrence of ionic crosslinking of the HPAM precursors, and the ultimate gelation time of each sample was the time that G' approaches to its plateau state (Fig. 4). The nHAp loaded sample showed a lower induction time with a higher initial and ultimate storage modulus of the hydrogel, which is assumed to be due to the polymer-nano particle interaction besides high molecular entanglement at the beginning of the test. In addition, incorporation of 50 wt. % nHAp accelerated the gelation of the HPAM solution. The crosslink densities of the optimum hydrogels (ν_{RH}) were also calculated, and results are presented in Table 2. The mechanical strength of the prepared and examined hydrogels were compared at their ultimate gelation. It is clearly observed that nHAp particles enhanced both ultimate gel modulus and crosslink density.

RSC Advances Accepted Manuscript

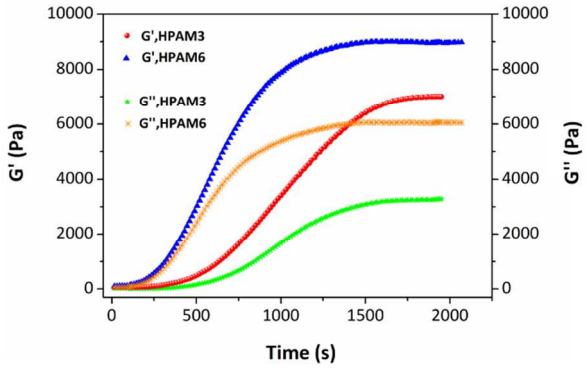

Fig. 4 Variation of storage and loss modulus (G' and G'') of HPAM3 and HPAM6 hydrogels as a function of time at 37 °C. Frequency of 0.1 Hz and a strain amplitude of 1% were applied.

Table 2. Numerical values of storage modulus (G′) and crosslink density (υ_{RH}) of the hydrogels corresponding to the optimized solutions.

Sample	G' (kPa)	Gelation time (min)	υ_{RH} (mol cm^{-3})
HPAM3	7	30	2.7e-06
HPAM6	9	18	3.49e-06

Atomic force microscopy scan of the hydrogels with higher Cr (III) concentration also exhibited higher Young's modulus and surface elasticity of the samples (Fig. 5A). It can be observed in Fig. 5B that nHAp loaded hydrogel demonstrated steeper slop force scan compared to the counterpart hydrogel, indicating its higher stiffness. Only the piezo extension data for the samples were examined in order to avoid errors obtained by tip adhesion during the approach–retraction cycles.

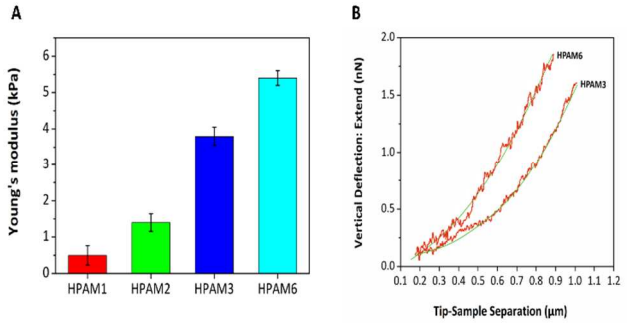

Fig. 5 Surface elastic modulus of the hydrogels with different crosslink densities. A) Young′s moduli of the HPAM hydrogels, B) Typical force-indentation curves (red curves) and fits to the Hertz model (green line) obtained for HPAM3 and HPAM6. The data were presented as the means ± standard deviation for n=3.

The result of water uptake experiment performed for the crosslinked hydrogels revealed that all the hydrogels reached the equilibrium swelling in less than 15 hours. As it is observed in Fig. 6A, water content of the hydrogels was inversely proportional to the Cr (III) level. However, increasing the level of nHAp led to the decrease of swelling degree compared to the unfilled counterpart hydrogel sample. Dissolution of HPAM hydrogels in water as a function of time was also followed for 30 days (Fig. 6B). The results showed that the amount of remained gel increased with the elevation of Cr (III) concentration and incorporation of nHAp.

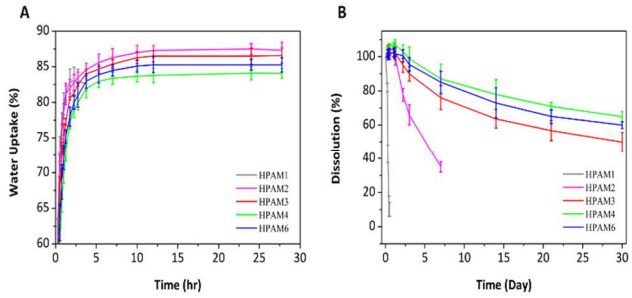

Fig. 6 A) Water uptake of the HPAM/Cr (III) hydrogels after 30 hours, B) Dissolution of HPAM/Cr (III) hydrogels exposed to water for 30 days at 37℃. Error bars show means± standard deviation for n=3.

The results of cell viability demonstrated that there were no serious cytotoxic effects on cells exposed to the HPAM hydrogels with Cr (III) concentration up to 0.2 wt. % (Figures. 7 A, B). Therefore, to have a hydrogel with both desirable biocompatibility and mechanical strength, 0.2 wt. % Cr (III) solution was considered as a threshold value to efficiently crosslink HPAM solutions (see supporting information for more detail (S-II)).
The representative SEM morphologies of the MScs also illustrate the spherical morphology for the cells after 3 days of culture in HPAM3 and HPAM6 (Fig. 7C). In both optimized hydrogels, the MSCs formed adhesion contacts on the hydrogel surfaces using filopodia, indicating a desirable cellular attachment (see supporting information for more detail (S-V)).

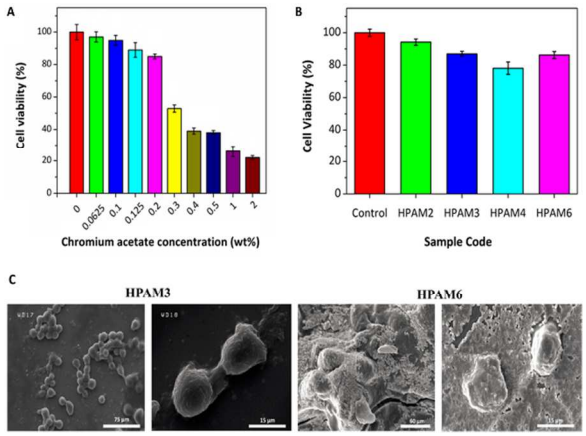

Fig. 7 Neutral red staining of MSCs after A) 1 day exposure to Cr (III) solutions and B) 7 days exposure to HPAM hydrogels in agar diffusion test. The data were presented as the means ± standard deviation for n=3. C) Scanning electron micrograph of the MSCs with initial cell density of 1×10^5 cells/ml cultured in the HPAM3 and HPAM6 after 3 days.

The safranin O and Alcian blue staining indicated that the cells attached to the HPAM3 hydrogel can secrete time dependent proteoglycan molecules and the highest amount appeared after

RSC Advances Accepted Manuscript

21 days (Fig. 8A, B). The results of GAG assay confirmed these findings, indicating chondrogenic differentiation of MSCs within the hydrogels (Fig. 8D). GAG determination also demonstrated that the encapsulated chondrocytes secreted higher amount of GAG than MSCs.

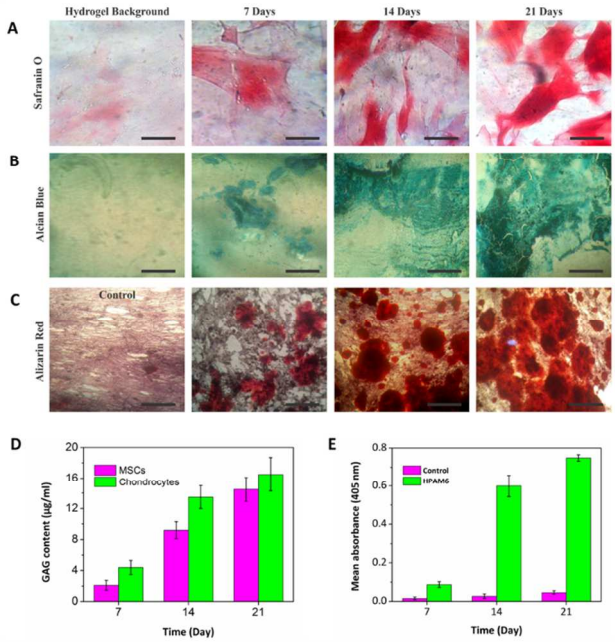

Fig. 8 A) Saffranin O, B) Alcian blue staining of MSCs encapsulated in the HPAM3 with Initial cell density of 10^6/ml, C) Alizarin Red staining of MSCs cultured in the presence of nHAp loaded hydrogel (HPAM6) and HPAM3 as a negative control in regular time intervals (Initial cell density: 5×10^2 cells/ml) (Scale bar represent 100 µm). D) Quantitative analysis of GAG content in the cultured scaffold, E) Quantification of Alizarin red staining of MSCs. Error bars represent means ± standard deviation for n=3.

As shown in Fig. 8C, the calcium deposition capacity of the MSCs exposed to the HPAM6 hydrogel extract followed an increasing trend by time with much more mineralization (deeply red precipitates) at 21 days cell culturing. Quantitative analysis of bone mineralization is also demonstrated in Fig. 8E. In addition, no indication of mineralization was observed for the cells cultured in the presence of HPAM3 hydrogel (as control) after 21 days.

The activity of the encapsulated MSCs was studied by performing gene expression test using Real time- PCR method. A significant increase in the expression of Col II and Aggrecan was revealed for MSCs encapsulated in HPAM3. In this group, the expression of Col II and Aggrecan were, respectively, 21.194 (P=0.03) and 8.229 (P<0.5) fold higher than the 2-D cultured stem cells as a control, while the expression of Col I was 0.323 (P<0.5) fold lower than the control at day 21 (Fig. 9A). The encapsulated chondrocytes within the HPAM3 also exhibited 1000.755 (P>0.05) and 77.373 (P=0.005) fold increase in Col II and Aggrecan gene expression, respectively, compared to the mono layer cultured chondrocytes (TCPS), while the expression of Col I was 0.02 (P>0.001) fold lower than the TCPS sample (Fig. 9B). However, after normalization to Col I, the MSCs, incorporated into the HPAM6 hydrogel, showed 14.717 (P=0.043) and 3.087 (P<0.001) fold increase in Runx2 and Osteopontin gene expression, respectively, with respect to the TCPS sample (Fig. 9C).

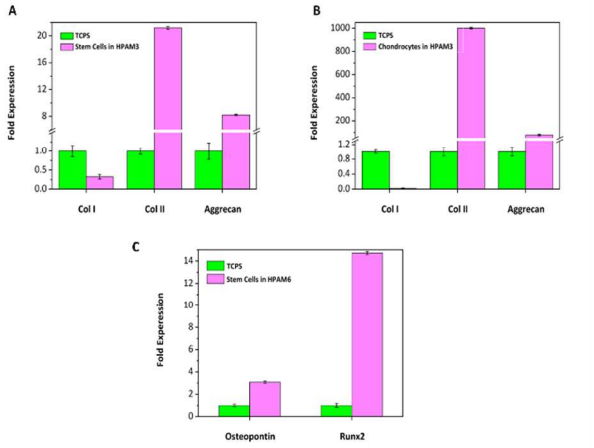

Fig. 9 Gene expression profile for MSCs cultured in HPAM hydrogels for 21 days. A, B) Chondrogenesis of MSCs and chondrocytes cultured in HPAM3 scaffold, C) Osteogenesis of MSCs encapsulated into the HPAM6 scaffold. The data were presented as the means ± standard deviation for n=3.

4. Discussion

In this study, a new biphasic injectable hydrogel based on HPAM and nHAp crosslinked by Cr (III) was successfully fabricated as a MSCs career for articular cartilage and subchondral bone reconstruction. In most cases, cartilage scaffolds would be unstable at the defect site due to the lack of adherence to the cartilage tissue and need to be sutured. However, the designed biphasic structure with one phase including nHAP provided integration of the scaffold to the subchondral bone and maintained the other phase remaining at the cartilage defect site without any suturing.

The results of gelation characterization showed that the HPAM concentration and Cr (III) level play important roles in tuning the onset of the gelation as well as rate of crosslink formation and hence the stiffness of the HPAM hydrogel (Fig. 2). It has been suggested that HPAM solutions can be crosslinked in the presence of Cr (III) due to the electrostatic interaction between negatively charged carboxylate groups and trivalent chromium acetate (Fig. 3A).[33,34] Hence, as the concentration of HPAM increased, the numbers of carboxylate anion on the back bone of the HPAM chains also increased, leading to the higher active sites for the Cr (III) ions as the crosslink agent. Moreover, increasing the HPAM concentration led to the increase in the number of physical entanglement between HPAM chains, which contributed to the enhancement of the gel stiffness. As the 5 wt. % HPAM solution comprising 0.2 wt. % Cr (III) lacked injectability, the 4 wt. % HPAM solution with similar amount of crosslink agent (HPAM3) found to be the optimum solution to be employed as injectable hydrogel scaffold. However, without preheating, the gelation time of HPAM3 was much higher, indicating the important role of the preheating on the gelation time. The level of Cr (III) also showed to be restricted by the cytotoxic effect of Cr (III) ion upon the cultured cells above 0.2 wt. % of Cr (III). Therefore, chromium acetate found to be a suitable crosslink agent for HPAM solution used for tissue regeneration purpose, providing the concentration of Cr (III) was kept below this critical level.

RSC Advances Accepted Manuscript

It is clearly seen in Fig. 4 that the elastic component of the modulus (G') increased by time, indicating the network formation via crosslinking of the HPAM chains by the Cr (III) ions. Moreover, as the crosslinked hydrogel is a viscoelastic network, hence crosslinking would also retard the viscous responses by the network towards the applied dynamic field. In fact, G' and G" control the ease of micromechanical responses by the scaffold towards the regenerating cells. As can be observed, inclusion of nHAp in the HPAM/Cr (III) solution led to the decrease of the gelation induction time as well as increase in the network elastic modulus. This fact may be attributed to the physical interactions between the nHAP and HPAM functional groups, leading to the higher extent of physical crosslinks and the longer polymer chains' relaxation time. The enhancement of the ultimate modulus by the nHAP is also obvious in Fig. 4, which implies that nHAP particles improved both bioactivity and strength of the formed gel network.[17,35] Gaharwar et al. showed that addition of nanohydroxyapatite to poly (ethylene glycol) precursor resulted in a hydrogel with higher extensibilities, toughness, fracture stresses than conventional PEG hydrogels, and they reported that the increase in mechanical properties was attributed to the polymer- nano particle interactions.[35]

AFM analysis also showed the increase in surface elastic modulus by increasing the chromium acetate concentration, which is consistent with increase in electrostatic interaction between Cr (III) ions and HPAM's carboxylate groups (Fig. 5). The impregnation of nHAp in the HPAM gel network also resulted in stiffening of the gel, indicating polymer- particle interaction.[36-38] Kim al. reported that poly(propylenefumarate)/ nHAp composite hydrogel exhibited a significant increase in Young's modulus compared with the counterpart hydrogel.[39]

The result of water uptake by the crosslinked HPAM hydrogels demonstrated that the rate of water absorption and degree of equilibrium swelling decreased by increasing the Cr (III) and nHAp concentration (Fig. 6A). This is attributed to the increase in the stiffness and elasticity of the hydrogel network, which limits the diffusion and absorption of the water molecules, as the network resists entropy loss by the penetration of the water molecules. Although it was expected that HPAM1 had the highest water uptake, it indicated the lower amount because of its too much loose network structure, contributing to the disintegration after a short time exposure to water. Moreover, in the nHAp loaded hydrogel, the particles have hydrophobic characteristics which reduce the affinity of the network for water absorption. These results have been argued by others for different hydrogels.[17,35,40] The results also showed that the higher chemical and physical crosslink density, the more resistance towards water dissolution (Fig. 6B).

According to cell viability results, to have a hydrogel with both desirable biocompatibility and mechanical strength, 0.2 wt. % Cr (III) solution was considered as a threshold value to efficiently crosslink HPAM solutions (Figures. 7A, B). Moreover, the spherical morphologies shown in SEM images for both ostegenic and chondrogenic differentiations are expected due to the 3D structure of HPAM hydrogels (Fig. 7C). Indeed, the cell morphology is a debatable subject and discrimination between cells with their morphologies is almost impossible. It has been well reported that the morphology (and also the phenotype) of the chondrocytes is changed from spherical to spindle in a monolayer culture. This morphology can be changed to spherical following culture in 3D hydrogels. For the osteoblasts, the morphology of the cells in the body, in 3D structure, is spherical and these cells also take the spindle morphology after seeding in monolayer culture. Despite of this change in osteoblast morphology, its phenotype remains almost constant (due to the mechanical stiffness of polystyrene tissue culture plate).

Alcian blue, safranin O and DMMB staining proved the expression of GAGs by encapsulated MSCs in the HPAM3 after 21 days (Fig. 8). In addition, this expression is higher for encapsulated chondrocytes than encapsulated MSCs after 21 days, indicating preserving their phenotype as a result of encapsulation.[41] It has been shown that no sign of GAG expression can be detected for the chondrocytes in monolayer culture since they lose their original phenotype.[42] Balakrishnan et al. showed chondrocytes encapsulated in self cross-linked oxidized alginate/gelatin hydrogel demonstrated viability, proliferation within the matrix, while preserving their phenotype. Moreover, for encapsulated MSCs compared with TCPS, the Real time-PCR results demonstrated the increase in expression of the main chondrocyte genes (Col II and Aggrecan) and the decrease in Col I (Fig. 9A).[10] Therefore, HPAM hydrogels can be considered as an effective material in cell encapsulation for preserving the chondrocyte phenotype and also differentiating to chondrocyte (Figures 9A, B).

In our investigation, mineralization of the nanocomposite constructs was confirmed by Alizarin red staining after 7, 14 and 21 days (Fig. 8C, E). The maximum amount of calcium deposition was obtained after 21 days. This is attributed to the nHAp incorporation into the scaffolds, which induce osteogenic differentiation.[14,39,43] Patel et al showed that impregnation of HAp nano particles in the cyclic acetal hydrogels motivated mineralization and alkaline phosphatase expression by incorporated rabbit MSCs.[43]. The results of Real time- PCR also indicated an augmentation in Runx2 and Osteopontin expression by the stem cells encapsulated in the HPAM6 compared to the TCPS sample when the samples were normalized to Col I (Fig. 9C). These results showed that the biological characteristics of the proposed hydrogel were engineered to play as an inductive material for bone regeneration. Although the stiffness of the final HPAM/nHAp hydrogels was less than the native bone, it showed to be a good support for osteogenic differentiation of mesenchymal stem cells. This was evidenced by Alizarin red staining and PCR-Real time experiments (Fig. 8C, E and 9C). In fact, HAp nano particles as the main component of the bone could compensate the low mechanical properties of the HPAM hydrogels and induce osteogenic differentiation.

5. Conclusion

The results of the present work showed that partially hydrolyzed polyacrylamide (HPAM) as a water soluble polymer has high potential for the preparation of injectable hydrogel as scaffold for tissue engineering purpose. A new biphasic hydrogel based on HPAM and nHAp was successfully synthesized with a favorable and supportive cellular environment for MSCs in vitro. The comparative studies of HPAM3 and HPAM6 as optimized hydrogel compositions using for biphasic preparation demonstrated the significant role of nHAp particles in enhancement of the mechanical properties of the scaffold, improving MSCs adhesion and stimulating osteogenic differentiation of the encapsulated MSCs in the HPAM6 over 21 days cell culturing. However, MSCs encapsulated in HPAM3 maintained a round morphology and indicated an up regulation of chondrocyte-specific genes such as collagen type II and Aggrecan over a 21-day culture period.

RSC Advances Accepted Manuscript

These results make the new biphasic hydrogel desired material for further study in orthopedic applications.

References

1. G. Versier and F. Dubrana, *Orthopaedics & Traumatology: Surgery & Research*, 2011, **97**, S140-S153.
2. R. J. Williams, *Operative Techniques in Orthopaedics*, 2006, **16**, 218-226.
3. G. Filardo, E. Kon, F. Perdisa, B. Di Matteo, A. Di Martino, F. Iacono, S. Zaffagnini, F. Balboni, V. Vaccari and M. Marcacci, *The Knee*, 2013, **20**, 570-576.
4. S. P. Nukavarapu and D. L. Dorcemus, *Biotechnology advances*, 2013, **31**, 706-721.
5. B. S. Dunkin and C. Lattermann, *Operative techniques in sports medicine*, 2013, **21**, 100-107.
6. M. Marcacci, G. Filardo and E. Kon, *Injury*, 2013, **44**, S11-S15.
7. J. Vaquero and F. Forriol, *Injury*, 2012, **43**, 694-705.
8. Z. Li and Z. Cui, *Biotechnology Advances*, 2014, **32**, 243-254.
9. N. Naveena, J. Venugopal, R. Rajeswari, S. Sundarrajan, R. Sridhar, M. Shayanti, S. Narayanan and S. Ramakrishna, *Journal of Materials Chemistry*, 2012, **22**, 5239-5253.
10. A. Au, J. Ha, A. Polotsky, K. Krzyminski, A. Gutowska, D. S. Hungerford and C. G. Frondoza, *Journal of Biomedical Materials Research Part A*, 2003, **67**, 1310-1319.
11. S. Bonakdar, S. H. Emami, M. A. Shokrgozar, A. Farhadi, S. A. H. Ahmadi and A. Amanzadeh, *Materials Science and Engineering: C*, 2010, **30**, 636-643.
12. M. Morille, T. Van-Thanh, X. Garric, J. Cayon, J. Coudane, D. Noël, M.-C. Venier-Julienne and C. N. Montero-Menei, *Journal of Controlled Release*, 2013, **170**, 99-110.
13. K. H. Bae, L.-S. Wang and M. Kurisawa, *Journal of Materials Chemistry B*, 2013, **1**, 5371-5388.
14. Q. Hu, Z. Tan, Y. Liu, J. Tao, Y. Cai, M. Zhang, H. Pan, X. Xu and R. Tang, *Journal of Materials Chemistry*, 2007, **17**, 4690-4698.
15. J. D. Kretlow, L. Klouda and A. G. Mikos, *Advanced drug delivery reviews*, 2007, **59**, 263-273.
16. L. Yu and J. Ding, *Chemical Society Reviews*, 2008, **37**, 1473-1481.
17. O. Im, J. Li, M. Wang, L. G. Zhang and M. Keidar, *Int J Nanomedicine*, 2012, **7**, 2087-2099.
18. M. R. Rogel, H. Qiu and G. A. Ameer, *Journal of Materials Chemistry*, 2008, **18**, 4233-4241.
19. J. Zhou, C. Xu, G. Wu, X. Cao, L. Zhang, Z. Zhai, Z. Zheng, X. Chen and Y. Wang, *Acta biomaterialia*, 2011, **7**, 3999-4006.
20. A. M. Getgood, S. J. Kew, R. Brooks, H. Aberman, T. Simon, A. K. Lynn and N. Rushton, *The Knee*, 2012, **19**, 422-430.
21. T. J. Levingstone, A. Matsiko, G. R. Dickson, F. J. O'Brien and J. P. Gleeson, *Acta Biomaterialia*, 2014, **10**, 1996-2004.
22. Q. Zhao, J. Sun, Y. Lin and Q. Zhou, *Reactive and Functional Polymers*, 2010, **70**, 602-609.
23. M. Yamamoto, K. Yanase and Y. Tabata, *Materials*, 2010, **3**, 2393-2404.
24. M. Sadat-Shojai, M.-T. Khorasani, E. Dinpanah-Khoshdargi and A. Jamshidi, *Acta Biomaterialia*, 2013, **9**, 7591-7621.
25. E. Hachet, H. Van Den Berghe, E. Bayma, M. R. Block and R. Auzély-Velty, *Biomacromolecules*, 2012, **13**, 1818-1827.
26. N. E. Kurland, Z. Drira and V. K. Yadavalli, *Micron*, 2012, **43**, 116-128.
27. O. Mashinchian, S. Bonakdar, H. Taghinejad, V. Satarifard, M. Heidari, M. Majidi, S. Sharifi, A. Peirovi, S. Saffar and M. Taghinejad, *ACS applied materials & interfaces*, 2014.
28. G. Repetto, A. del Peso and J. L. Zurita, *Nature protocols*, 2008, **3**, 1125-1131.
29. A. Ignatius and L. E. Claes, *Biomaterials*, 1996, **17**, 831-839.
30. M. A. Shokrgozar, S. Bonakdar, M. M. Dehghan, S. H. Emami, L. Montazeri, S. Azari and M. Rabbani, *Journal of Materials Science: Materials in Medicine*, 2013, **24**, 2449-2460.
31. C. A. Gregory, W. Grady Gunn, A. Peister and D. J. Prockop, *Analytical Biochemistry*, 2004, **329**, 77-84.
32. L. Montazeri, J. Javadpour, M. A. Shokrgozar, S. Bonakdar and S. Javadian, *Biomedical Materials*, 2010, **5**, 045004.
33. R. Jain, C. S. McCool, D. W. Green, G. P. Willhite and M. J. Michnick, SPE/DOE Symposium on Improved Oil Recovery, 2004.
34. R. Zolfaghari, A. A. Katbab, J. Nabavizadeh, R. Y. Tabasi and M. H. Nejad, *Journal of Applied Polymer Science*, 2006, **100**, 2096-2103.
35. A. K. Gaharwar, S. A. Dammu, J. M. Canter, C.-J. Wu and G. Schmidt, *Biomacromolecules*, 2011, **12**, 1641-1650.
36. L. Jianguo, Z. Li, Z. Yi, W. Huanan, L. Jidong, Z. Qin and L. Yubao, *Journal of biomaterials applications*, 2009, **24**, 31-45.
37. G. Wei and P. X. Ma, *Biomaterials*, 2004, **25**, 4749-4757.
38. L. Zhang, J. Rodriguez, J. Raez, A. J. Myles, H. Fenniri and T. J. Webster, *Nanotechnology*, 2009, **20**, 175101.
39. K. Kim, D. Dean, A. Lu, A. G. Mikos and J. P. Fisher, *Acta biomaterialia*, 2011, **7**, 1249-1264.
40. J. L. Wang, Y. A. Zheng and A. Q. Wang, *Advanced Materials Research*, 2010, **96**, 227-232.
41. R. Jin, L. Moreira Teixeira, P. J. Dijkstra, M. Karperien, C. Van Blitterswijk, Z. Zhong and J. Feijen, *Biomaterials*, 2009, **30**, 2544-2551.
42. F. Martin, M. Lehmann, P. Schläger, U. Sack and U. Anderer, *J Biochip Tissue chip S*, 2012, **2**, 2153-0777.
43. M. Patel, K. J. Patel, J. F. Caccamese, D. P. Coletti, J. J. Sauk and J. P. Fisher, *Journal of Biomedical Materials Research Part A*, 2010, **94A**, 408-418.

RSC Advances Accepted Manuscript

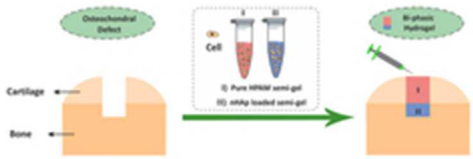

19x7mm (300 x 300 DPI)

RSC Advances Accepted Manuscript